# Microwave Spectrum, Conformational Equilibria and Intramolecular Hydrogen Bonding of 1-Amino-3-butene

K.-M. Marstokk and Harald Møllendal*

Department of Chemistry, The University of Oslo, P.O. Box 1033, Blindern, N-0315 Oslo 3, Norway

Marstokk, K.-M. and Møllendal, H., 1988. Microwave Spectrum, Conformational Equilibria and Intramolecular Hydrogen Bonding of 1-Amino-3-butene. – Acta Chem. Scand., Ser. A 42: 374–390.

The microwave spectrum of $H_2NCH_2CH_2CH=CH_2$ has been investigated in the 22.0–38.0 GHz spectral region at −50°C. Five low-energy conformers are believed to exist for this compound, four of which were assigned in this work. The rotamers denoted *Gauche I* and *Gauche II* each possess an intramolecular hydrogen bond formed between one of the amino group hydrogen atoms and the π electrons of the double bond, while *Extended I* and *Extended II* do not have this kind of stabilizing interaction. *Gauche I* is the most stable, being 0.8(3) kJ mol$^{-1}$ more stable than *Gauche II*, 1.9(5) kJ mol$^{-1}$ more stable than *Extended I*, and 2.1(5) kJ mol$^{-1}$ more stable than *Extended II*.

The hydrogen-bond strength in *Gauche I* and in *Gauche II* is compared with those in $HOCH_2CH_2CH=CH_2$ and $HSCH_2CH_2CH=CH_2$. The hydrogen-bond strength in *Gauche I* and in *Gauche II* of $H_2NCH_2CH_2CH=CH_2$ are each nearly the same as in $HSCH_2CH_2CH=CH_2$, but considerably weaker than in $HOCH_2CH_2CH=CH_2$.

**Dedicated to Professor Otto Bastiansen on his 70th birthday**

A large number of conformations produced by rotation around the C2–C3, C3–C4 and C4–N single bonds (see Fig. 1) is possible for 1-amino-3-butene. Figs. 2 and 3 show Newman projections of six selected rotamers.

It is known that ethylamine derivatives of the type $H_2NCH_2CH_2X$, where X is some proton-accepting atom or group, prefer two heavy-atom *gauche* conformations, each with an intramolecular hydrogen bond (H bond) formed between one of the amino group hydrogen atoms and the substituent X, as their most stable conformers. This has been found in recent microwave (MW) studies of $H_2NCH_2CH_2F$,[1] $H_2NCH_2CH_2C{\equiv}N$[2], $H_2NCH_2CH_2C{\equiv}CH$,[3] $H_2NCH_2CH_2NH_2$[4] and $H_2NCH_2CH_2OCH_3$.[5,6] The two heavy-atom *gauche* rotamers which are capable of forming intramolecular H bonds between one of the amino group hydrogen atoms and the π electrons of the double bond are denoted *Gauche I* and *Gauche II*, respectively, and are shown in Figs. 2 and 3. *Gauche III* of the same figures cannot have an internal H bond. It was found in this work that the H-bonded conformers *Gauche I* and *Gauche II* are the two preferred forms of 1-amino-3-butene, with *Gauche I* slightly more stable than *Gauche II*. This is in accord with findings for the other $H_2NCH_2CH_2X$-type molecules.[1–6]

In addition to the H-bonded *Gauche I* and *Gauche II* conformers, further rotamers might coexist with them. A MW study of the closely related alcohol, $HOCH_2CH_2CH=CH_2$,[7] led to the conclusion that its H-bonded conformer, which was the only one found, is at least 3 kJ mol$^{-1}$ more stable than any further hypothetical form of this molecule. However, the corresponding thiol, $HSCH_2CH_2CH=CH_2$,[8] revealed the existence of two *extended* conformers in addition to the more stable H-bonded *gauche* conformer. The internal H bond in amines is generally somewhat weaker than in the corresponding alcohols.

*To whom correspondence should be addressed.

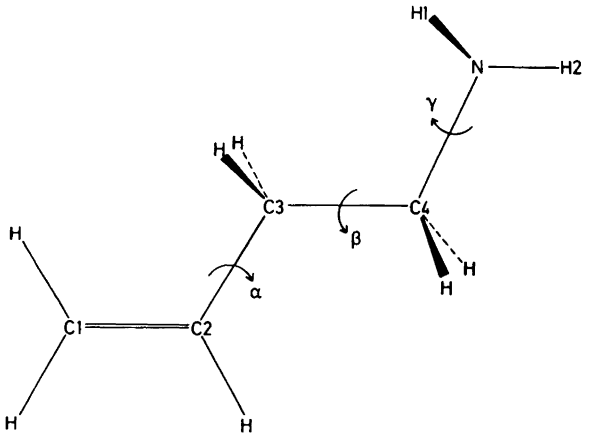


*Fig. 1.* Atom numbering and dihedral angles $\alpha = \angle C1C2C3C4$, $\beta = \angle C2C3C4N$, $\gamma = \angle C3C4NH2$. The conformation shown has $\alpha = \beta = \gamma = 0°$. Rotation around $\alpha$ by about 60°, $\beta$ by approximately 120° and $\gamma$ by about 0° in the direction indicated by the arrows produces the H-bonded *Gauche I* conformer. Keeping $\alpha$ and $\beta$ constant at these values, a further rotation around $\gamma$ by approximately 120° yields the other H-bonded *Gauche II*, while a rotation by 240° produces the non-H-bonded *Gauche III* rotamer. Rotation about $\alpha$ by 60°, $\beta$ by 0° and $\gamma$ by 0° yields *Extended I*. If a 120° rotation around $\gamma$ is then made, *Extended II* will result, whereas a 240° rotation around $\gamma$ results in *Extended III*.

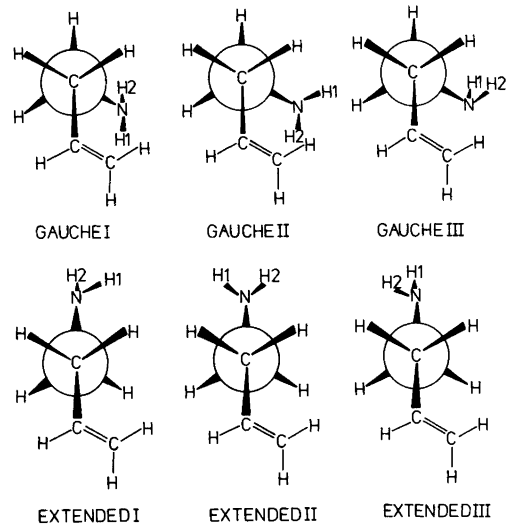


*Fig. 2.* Newman projections of the *gauche* and *extended* conformations of 1-amino-3-butene viewed along the C3–C4 bond.

It was therefore presumed that *extended* conformations might also be observable in the case of 1-amino-3-butene. This was found to be the case, as elucidated below.

1-Amino-3-butene, $H_2NCH_2CH_2CH = CH_2$, was chosen for study because we wanted to investigate the possible H bond interaction between the amino group and the $\pi$ electrons of the double bond. As mentioned above, it is generally found that alcohols form stronger internal H bonds than do the corresponding amines. Whether amines form stronger bonds than their thiol counterparts is not yet entirely clear. Comparison of intramolecular H bonding in $H_2NCH_2CH_2CH=CH_2$ with that in $HOCH_2CH_2CH=CH_2$ and $HSCH_2CH_2CH=CH_2$ might therefore shed light on this question.

## Experimental

1-Amino-3-butene was donated by Professor G. Courtois, Laboratoire de Synthese Organique, Université de Poitiers, France. The synthesis is described by him and his coworkers in Ref. 9. The sample was purified by gas chromatography before use. The spectrometer is an improved version of the one described briefly in Ref. 10 employing klystrons as microwave sources. With this equipment, quadrupole fine-structure splittings larger than approximately 0.6 MHz were resolved in favourable cases. The radio frequency microwave double resonance technique (RFMWDR) was used, as described by Wodarczyk and Wilson.[11] A Hewlett-Packard 8660A synthesized-signal generator with an ENI 503L RF power amplifier and a Hewlett-Packard 10514A mixer were utilized in the double resonance ex-

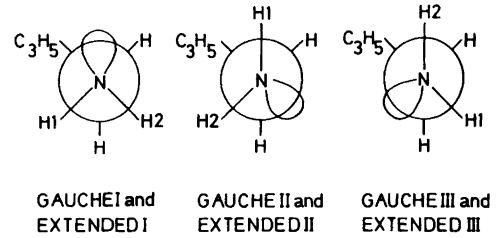


*Fig. 3.* Newman projections of the *gauche* and *extended* conformations of 1-amino-3-butene viewed along the N–C4 bond.

*Table 1.* Predicted principal axes bond-moment components calculated by the bond-moment method[a] for $H_2NCH_2CH_2CH{=}CH_2$.

| Conformation | $\mu_a/10^{-30}$ C m | $\mu_b/10^{-30}$ C m | $\mu_c/10^{-30}$ C m |
|---|---|---|---|
| *Gauche I* | 0.4 | 1.2 | 4.1 |
| *Gauche II* | 3.6 | 1.0 | 1.8 |
| *Gauche III* | 3.4 | 0.3 | 2.3 |
| *Extended I* | 0.8 | 0.2 | 4.0 |
| *Extended II* | 1.2 | 3.3 | 2.0 |
| *Extended III* | 1.9 | 2.3 | 3.1 |

[a]Ref. 13. 1 Debye = $3.33564\times10^{-30}$ C m.

periments. Measurements were made in the 22.0–38.0 GHz spectral region with the cell cooled with dry ice to about −50 °C. A study at lower temperatures could not be made because of insufficient vapour pressure of the compond. The pressure was 0.5–2 Pa during the spectral measurements. Relative intensity measurements were made largely as described in Ref. 12.

## Results

*Spectrum.* The MW spectrum of 1-amino-3-butene is very dense, with absorptions occurring every few MHz throughout the entire investigated MW region. It is also comparatively weak. The strongest lines, which turned out to be the ground-state *Q*-branch *c*-type transitions of *Gauche I* with *J* between 15 and 40, have peak absorption coefficients somewhat less than $3\times10^{-7}$ cm$^{-1}$. The $J = 6 \leftarrow 5$ *R*-branch *a*-type transitions of *Gauche II,* which were the strongest ones observed for this rotamer, are even somewhat weaker than this. The strongest transitions of *Extended I* and *Extended II* have peak absorption intensities less than $1\times10^{-7}$ cm$^{-1}$.

*Table 2.* Predicted[a] diagonal elements of the $^{14}$N-quadrupole coupling tensor for $H_2NCH_2CH_2CH{=}CH_2$.

| Conformation | $\chi_{aa}$/MHz | $\chi_{bb}$/MHz |
|---|---|---|
| *Gauche I* | 2.0 | 1.9 |
| *Gauche II* | −2.9 | 1.8 |
| *Gauche III* | −1.2 | 0.6 |
| *Extended I* | 1.8 | 1.9 |
| *Extended II* | −0.6 | −0.3 |
| *Extended III* | 2.0 | −1.2 |

[a]See text.

*Assignment of* Gauche I. Preliminary rotational constants of the three *gauche* as well as of the three *extended* conformations shown in Figs. 2 and 3 were computed by combining structural parameters taken from related molecules (see Table 14 below). Principal axis dipole moment components predicted by the bond-moment method[13] are useful for making definite assignments in cases like this. A computation of these parameters was therefore carried out, and the results are collected in Table 1. Likewise, the diagonal elements of the principal axis $^{14}$N-quadrupole coupling tensor of the nitrogen nucleus can be used to help identify the various conformers possessing similar rotational constants or dipole moments. The values shown in Table 2 have been computed as described in Ref. 14 assuming the principal quadrupole coupling constant of the $^{14}$N nucleus to be $\chi_z = -4.1$ MHz, the value found for $NH_3$,[15] and to be oriented 109.47° with respect to the three bonds to the nitrogen nucleus.

A preliminary set of rotational constants was calculated for *Gauche I.* This conformer was predicted (Table 1) to have its predominant principal axis dipole moment component along the *c*-axis. For a prolate asymmetrical rotor with Ray's asymmetry parameter[16] $\kappa$ close to −0.84, as in the present case, strong *Q*-branch *c*-type transitions will dominate throughout the investigated spectral range (22–38 GHz). The quadrupole coupling constants of Table 2 predict most of these transitions to be split into three strong components with a characteristic intensity pattern. Two

*Table 3.* Selected transitions of the ground vibrational state of the hydrogen-bonded *Gauche I* conformer of $H_2NCH_2CH_2CH{=}CH_2$.

| Transition | Observed frequency[a,b]/MHz | Obs−calc frequency/MHz | Centrifugal distortion | |
|---|---|---|---|---|
| | | | Total/MHz | Sextic/MHz |
| *b*-type | | | | |
| $10_{3,7} \leftarrow 10_{2,8}$ | 25537.11 | −0.03 | 17.68 | −0.02 |
| $12_{3,9} \leftarrow 12_{2,10}$ | 23993.95 | −0.04 | 17.53 | −0.04 |
| $13_{3,10} \leftarrow 13_{2,11}$ | 23909.03 | 0.00 | 10.99 | −0.05 |
| $14_{3,11} \leftarrow 14_{2,12}$ | 24431.62 | −0.02 | −1.81 | −0.05 |
| $15_{3,12} \leftarrow 15_{2,13}$ | 25637.23 | −0.06 | −22.23 | −0.05 |
| $16_{3,13} \leftarrow 16_{2,14}$ | 27571.46 | 0.11 | −51.32 | −0.04 |
| $15_{4,11} \leftarrow 15_{3,12}$ | 34830.24 | −0.03 | 71.08 | −0.14 |
| $16_{4,12} \leftarrow 16_{3,13}$ | 33343.07 | 0.03 | 74.57 | −0.18 |
| $17_{4,13} \leftarrow 17_{3,14}$ | 32216.38 | −0.03 | 68.90 | −0.22 |
| $18_{4,14} \leftarrow 18_{3,15}$ | 31610.57 | −0.03 | 51.23 | −0.25 |
| $19_{4,15} \leftarrow 19_{3,16}$ | 31654.96 | −0.12 | 19.16 | −0.26 |
| $20_{4,16} \leftarrow 20_{3,17}$ | 32443.87 | −0.15 | −29.15 | −0.24 |
| $21_{4,17} \leftarrow 21_{3,18}$ | 34035.24 | −0.01 | −94.73 | −0.18 |
| $22_{4,18} \leftarrow 22_{3,19}$ | 36448.13 | 0.19 | −177.17 | −0.08 |
| *c*-type | | | | |
| $4_{3,2} \leftarrow 4_{2,2}$ | 31063.31 | 0.04 | −1.86 | |
| $6_{3,4} \leftarrow 6_{2,4}$ | 29860.93 | −0.01 | 2.75 | |
| $8_{3,6} \leftarrow 8_{2,6}$ | 27337.48 | −0.01 | 11.80 | |
| $10_{3,8} \leftarrow 10_{2,8}$ | 23508.90 | −0.03 | 26.68 | −0.02 |
| $13_{4,10} \leftarrow 13_{3,10}$ | 37232.05 | −0.13 | 58.81 | −0.07 |
| $15_{4,12} \leftarrow 15_{3,12}$ | 32140.91 | 0.04 | 104.72 | −0.16 |
| $18_{4,15} \leftarrow 18_{3,15}$ | 22633.83 | −0.03 | 186.01 | −0.39 |
| $21_{5,17} \leftarrow 21_{4,17}$ | 37477.42 | 0.09 | 338.41 | −0.97 |
| $23_{5,19} \leftarrow 23_{4,19}$ | 29633.92 | 0.08 | 452.98 | −1.48 |
| $28_{6,23} \leftarrow 28_{5,23}$ | 37290.63 | −0.10 | 927.02 | −4.35 |
| $30_{6,25} \leftarrow 30_{5,25}$ | 27970.20 | 0.13 | 1082.36 | −5.60 |
| $35_{7,29} \leftarrow 35_{6,29}$ | 35106.50 | −0.07 | 1957.41 | −13.49 |
| $36_{7,30} \leftarrow 36_{6,30}$ | 29951.57 | 0.05 | 2029.60 | −14.58 |
| $2_{2,1} \leftarrow 1_{1,1}$ | 30870.28 | 0.01 | −0.67 | |
| $3_{2,2} \leftarrow 2_{1,2}$ | 37269.17 | 0.06 | −0.51 | |
| $8_{1,7} \leftarrow 7_{2,5}$ | 32474.39 | 0.02 | −11.33 | 0.01 |
| $10_{0,10} \leftarrow 9_{1,8}$ | 31800.29 | 0.09 | 9.56 | 0.04 |
| $12_{2,11} \leftarrow 11_{3,9}$ | 32376.57 | −0.14 | −17.34 | 0.10 |
| $14_{4,11} \leftarrow 13_{5,9}$ | 27101.98 | −0.02 | −59.47 | 0.15 |
| $17_{5,12} \leftarrow 16_{6,10}$ | 33557.14 | 0.01 | −127.71 | 0.40 |
| $17_{5,13} \leftarrow 16_{6,11}$ | 32860.47 | −0.08 | −112.87 | 0.39 |
| $21_{7,14} \leftarrow 20_{8,12}$ | 31243.42 | 0.04 | −187.29 | 0.81 |
| $21_{7,15} \leftarrow 20_{8,13}$ | 31210.40 | −0.04 | −185.72 | 0.80 |
| $26_{9,17} \leftarrow 25_{10,15}$ | 35643.70 | −0.05 | −333.81 | 2.10 |
| $26_{9,18} \leftarrow 25_{10,16}$ | 35641.43 | 0.01 | −333.59 | 2.10 |
| Coalescing $K_{-1}$-lines[c] | | | | |
| $32_{12} \leftarrow 31_{13}$ | 33044.23 | −0.04 | −507.88 | 3.94 |
| $38_{15} \leftarrow 37_{16}$ | 30518.61 | 0.02 | −708.09 | 6.18 |
| $45_{18} \leftarrow 44_{19}$ | 33952.83 | 0.06 | −1125.26 | 12.99 |
| $51_{21} \leftarrow 50_{22}$ | 31387.31 | 0.11 | −1414.44 | 16.46 |

[a] ±0.10 MHz. [b] Corrected for $^{14}N$ quadrupole interaction; see text. [c] The $K_{-1}$-energy doublets coalesce for high values of $K_{-1}$. Subscripts of $J$ quantum number refer to $K_{-1}$.

*Table 4.* Spectroscopic constants[a,b] for the hydrogen-bonded *Gauche I* conformer of $H_2NCH_2CH_2CH{=}CH_2$.

| Vib. state | Ground | First ex. C2−C3 tors. | First ex. C3−C4 tors.[e] |
|---|---|---|---|
| N.o.t.[c] | 112 | 74 | 32 |
| R.m.s.[d]/MHz | 0.072 | 0.096 | 0.105 |
| $A_v$/MHz | 9223.8669(49) | 9289.447(10) | 9249.250(27)[f] |
| $B_v$/MHz | 3199.3397(20) | 3193.9278(36) | 3191.2672(69)[f] |
| $C_v$/MHz | 2668.2862(18) | 2662.8728(32) | 2662.4970(84)[f] |
| $\Delta_J$/kHz | 4.4255(70) | 4.140(13) | 4.4255[g] |
| $\Delta_{JK}$/kHz | −28.581(22) | −27.452(47) | −28.92(29) |
| $\Delta_K$/kHz | 75.891(87) | 75.504(35) | 78.8(28) |
| $\delta_J$/kHz | 1.4216(15) | 1.3200(15) | 1.437(12) |
| $\delta_K$/kHz | 6.704(65) | 7.54(21) | 7.19(90) |
| $\Phi_J$/Hz | 0.063(11) | −0.0050(23) | −[h] |
| $\Phi_{JK}$/Hz | −0.571(35) | −0.2124(61) | −0.772(61) |
| $\Phi_{KJ}$/Hz | 2.97(69) | −1.21(10) | 6.4(13) |
| $\Phi_K^j$/Hz | −3.5(12) | 3.13(14) | −[h] |

[a]Uncertainties represent one standard deviation. [b]*A*-reduction *I*′-representation. [c]Number of transitions. [d]Root-mean-square deviation. [e]Could alternatively be the first excited vibrational state of the lowest bending mode. [f]Based on tentative assignment of one *R*-branch line; see text. $A_v - C_v = 6586.753(28)$ MHz and $\varkappa = -0.839444$ are definite. [g]Kept constant at the ground-state value shown in the second column of this table. [h]Kept constant at zero in the least-squares fit. [i]Further sextic centrifugal distortion constants kept at zero; see text.

*Table 5.* $^{14}$N-quadrupole splittings[a] ($E_q$) and diagonal elements of the quadrupole coupling tensor of the *Gauche I* conformer of $H_2NCH_2CH_2CH{=}CH_2$.

| Transition | $F' \leftarrow F$ | $E_q$(obs)/MHz | $E_q$(obs)−$E_q$(calc)/MHz |
|---|---|---|---|
| $2_{2,1} \leftarrow 1_{1,1}$ | 3 ← 2 | 0.29(3) | 0.04 |
| | 2 ← 1 | −1.05(3) | 0.00 |
| | 1 ← 0 | 1.67(4) | 0.08 |
| $4_{1,3} \leftarrow 3_{0,3}$ | 5 ← 4 | 0.34(3) | 0.01 |
| | 4 ← 3 | −0.90(3) | 0.08 |
| $6_{3,3} \leftarrow 6_{2,5}$ | 7 ← 7 | 0.18(4) | 0.03 |
| | 5 ← 5 | | −0.07 |
| | 6 ← 6 | −0.43(4) | −0.04 |
| $16_{4,13} \leftarrow 16_{3,13}$ | 17 ← 17 | −0.28(3) | 0.00 |
| | 15 ← 15 | | 0.05 |
| | 16 ← 16 | 0.41(3) | −0.10 |
| $17_{4,14} \leftarrow 17_{3,14}$ | 18 ← 18 | −0.24(3) | 0.00 |
| | 16 ← 16 | | 0.04 |
| | 17 ← 17 | 0.63(3) | 0.12 |
| $18_{4,15} \leftarrow 18_{3,15}$ | 19 ← 19 | −0.30(3) | −0.07 |
| | 17 ← 17 | | −0.03 |
| | 18 ← 18 | 0.45(3) | −0.05 |
| $23_{5,19} \leftarrow 23_{4,19}$ | 24 ← 24 | −0.14(3) | 0.12 |
| | 22 ← 22 | | 0.09 |
| | 23 ← 23 | 0.54(3) | 0.06 |

$^{14}$N quadrupole coupling constants/MHz
$\chi_{aa} = 2.07(40)$ $\chi_{bb} = 2.14(24)$

[a]Uncertainties represent one standard deviation.

of these components lie so close together that it is not possible to resolve them with our instrument. However, these two components are in most cases split from the third by 0.4–0.7 MHz, which is approximately the limit of our resolution. The observed split lines (or "shoulders") were quite useful in making the first assignments of the strong *c*-type *Q*-branch lines of this conformer. These assignments were gradually extended to include *c*-type *R*-branch as well as the rather weak *b*-type *Q*-branch transitions. No *a*- or *b*-type *R*-branch lines were assigned with certainty, presumably because of insufficient intensities caused by small dipole moment components, as demonstrated below in the section on dipole moment determination. A total of approximately 130 transitions were ultimately assigned for *Gauche I*. Some selected transitions are listed in Table 3 (the complete spectra are available from the authors upon request, or from the Molecular Spectra Data Center, Bldg. 221, Room B 268, National Bureau of Standards, Gaithersburg, Maryland 20899, U.S.A., where they have been deposited). 112 transitions were used to determine the spectroscopic constants shown in Table 4. Sextic centrifugal distortion constants had to be employed in order to obtain a good fit. Four of them were sufficient to obtain a root-mean-square deviation comparable to the experimental uncertainty (see Table 4). However, these sextic constants are quite uncertain and also highly correlated.

Some of the transitions appearing in Table 3 were split by quadrupole interaction of the $^{14}N$ nucleus, while "shoulders" were observed on others. Small frequency shifts of the peaks which were measured occur for still other transitions. In order to arrive at as accurate spectroscopic constants as possible, the transitions in question were "corrected" for quadrupole interaction. The quadrupole coupling constants shown in Table 5 were used for this purpose. The transitions appearing in Table 3 have been "corrected" in some cases and the frequencies shown there may deviate slightly from the observed frequencies.

A problem was encountered during the fitting of high-$J$ $^cQ$-branch lines to the ordinary Watson *A*-reduction $I^r$-representation Hamiltonian.[17] Several such lines, starting with the $37_{7,31} \leftarrow 37_{6,31}$ transition, were found to deviate from their predicted frequencies (there is no doubt about the assignments of these transitions). The reason for these deviations, which vary from about 0.5 MHz up to a few MHz, is difficult to say. Perhaps some kind of Coriolis interaction with low-lying levels in the potential surface can account for this behaviour. Interestingly, the high-$J$, high-$K_{-1}$ *R*-branch lines do not display this kind of interaction, as shown by a few examples listed in Table 3.

*$^{14}N$-nuclear quadrupole coupling constants.* The selected transitions appearing in Table 5 were used to determine the quadrupole coupling constants of the $^{14}N$ nucleus following the procedure of Ref. 18. The resulting constants $\chi_{aa} = 2.07(40)$ MHz and $\chi_{bb} = 2.14(24)$ MHz (Table 5) compare favourably with the predicted values of $\chi_{aa} = 2.0$ MHz and $\chi_{bb} = 1.9$ MHz of Table 2. This is independent evidence that the assigned conformer is indeed *Gauche I*.

*Vibrationally excited states.* The ground state transitions were accompanied by a satellite spectrum presumably belonging to vibrationally excited states of *Gauche I*. Two such states were assigned, as shown in Table 4. The strongest of these satellites had approximately 50% of the intensity of the ground state at about −50 °C. The $^bQ$-transitions were too weak to be assigned with certainty for this excited state. Several of the measured transitions were split or perturbed a little by quadrupole interaction, just as in the case of the ground vibrational state. It was not possible to determine the $^{14}N$-quadrupole coupling constants with high precision. The ground state values of the quadrupole coupling constants were therefore utilized in "correcting" some of the 74 transitions used to determine the spectroscopic constants listed in Table 4. Interestingly, there were no problems similar to those found for the ground state, with the least-squares fitting of the high-$J$ *Q*-branch of both the two excited states shown in Table 4.

Relative intensity measurements[12] yielded a frequency 95(20) $cm^{-1}$ for this vibration, which was assumed to be the first excited state of the torsion around the C2–C3 bond. This is close to 93(4) $cm^{-1}$ determined from the corresponding frequency of *skew*-1-butene,[19] 84(20) $cm^{-1}$ found for 3-buten-1-ol,[7] and 85(20) $cm^{-1}$ found for 3-butene-1-thiol,[8] as expected.

The second strongest satellite spectrum had about 40% of the ground-state intensity. Un-

fortunately, it was not possible for us to make definite assignments of the *c*-type *R*-branch transitions of this excited state, because there were only some few comparatively weak low-*J*- transitions of this kind in the spectrum. The spectroscopic constants of Table 4 have been derived using only one $^cR$-line, namely the $8_{1,7} \leftarrow 7_{2,5}$ at 32290.86 MHz. However, from the many $^cQ$-branch transitions assigned in this case, $A_v - C_v$ = 6586.753(28) MHz and $\kappa = -0.839444$ were determined. "Correction" for quadrupole interaction was made in the same manner as above.

A frequency of 139(30) $cm^{-1}$ was determined by relative intensity measurements[12] for this fundamental, which is presumed to be the C3–C4 torsional vibration or perhaps the lowest heavy-atom bending mode. 172(15) $cm^{-1}$ was found by relative intensity measurements for this fundamental mode in 3-buten-1-ol,[7] while 137(30) $cm^{-1}$ was determined for 3-butene-1-thiol.[8]

*Dipole moment.* It is necessary to know the dipole moment in order to determine energy differences between conformers. It is also useful to know the dipole moment in order to differentiate between conformations with very similar rotational constants. Unfortunately, we were only able to find transitions with resolved Stark effects which were practically independent of $\mu_b$. Therefore, only $\mu_a$ and $\mu_c$ could be determined. The results found following the standard procedure of Ref. 18 are shown in Table 6. In order to calculate the total dipole moment of this conformer, $\mu_b$ was assigned the value $1.18 \times 10^{-30}$ C m calculated by the bond-moment method.[13]

Comparison of the experimental *a*- and *c*-axis dipole moment components of Table 6 with those predicted[13] (Table 1) for *Gauche I* show good agreement. This too is evidence for the assignment of this spectrum to the said conformer.

*Assignment of* Gauche II. In analogy with the other ethylamine derivatives referred to in the introductory section,[1-6] the H-bonded *Gauche II* conformer was presumed to have nearly the same internal energy as *Gauche I.* A large fraction of *Gauche II* was therefore presumed to be present. As shown in Table 1, this rotamer was estimated to possess a relatively large *a*-axis dipole moment component. A search was therefore first made for the strong low-*J* *R*-branch transitions, which were soon found. Some of the assignments were confirmed using the RFMWDR technique.[11] The considerably weaker *b*- and *c*-type lines were subsequently assigned. Selected transitions are listed in Table 7. No transitions displayed quadrupole splittings. The predicted quadrupole coupling constants shown in Table 2 for this rotamer predict splittings which are considerably less than the resolution of our spectrometer. About 90 transitions were assigned for *Gauche II,* 82 of which were used to determine the spectroscopic constants listed in Table 8. High-*J* *c*-type transitions (Table 7) were employed in the least-squares determinations of the entries of Table 8. No problems were encountered in the fitting procedure for these transitions, as opposed to the situation for the ground vibrational state of *Gauche I,* as described above.

*Table 6.* Stark coefficients[a] and dipole moment[a] of the *Gauche I* conformer of $H_2NCH_2CH_2CH{=}CH_2$.

| Transition | | $\Delta\nu\ E^{-2}/10^{-5}$ MHz $V^{-2}$ $cm^2$ | |
|---|---|---|---|
| | | Obs | Calc |
| $6_{3,4} \leftarrow 6_{2,4}$ | $\lvert M\rvert = 6$ | −2.06(3) | −2.02 |
| | $\lvert M\rvert = 5$ | −1.48(2) | −1.46 |
| | $\lvert M\rvert = 4$ | −0.960(15) | −1.00 |
| $8_{3,5} \leftarrow 8_{2,7}$ | $\lvert M\rvert = 8$ | −0.517(7) | −0.515 |
| $9_{3,6} \leftarrow 9_{2,8}$ | $\lvert M\rvert = 9$ | −1.00(2) | −1.01 |
| Dipole moment/$10^{-30}$ C m | | | |
| $\mu_a$ = 0.751(6) | $\mu_b$ = 1.18[b] | $\mu_c$ = 3.660(30) | $\mu_{tot}$ = 3.92(4) |

[a]Uncertainties represent one standard deviation. [b]Assumed; see text. 1 Debye = $3.33564 \times 10^{-30}$ C m.

*Table 7.* Selected transitions of the ground vibrational state of the hydrogen-bonded *Gauche II* conformer of $H_2NCH_2CH_2CH{=}CH_2$.

| Transition | Observed frequency[a,b]/MHz | Obs−calc frequency/MHz | Centrifugal distortion | |
|---|---|---|---|---|
| | | | Total/MHz | Sextic/MHz |
| *a*-type | | | | |
| $4_{0,4} \leftarrow 3_{0,3}$ | 22835.40 | −0.07 | −0.88 | |
| $4_{1,3} \leftarrow 3_{1,2}$ | 24077.32 | −0.03 | −1.22 | |
| $4_{1,4} \leftarrow 3_{1,3}$ | 22069.60 | −0.05 | −0.42 | |
| $4_{2,2} \leftarrow 3_{2,1}$ | 23410.77 | 0.10 | −0.40 | |
| $4_{2,3} \leftarrow 3_{2,2}$ | 23111.75 | 0.09 | −0.17 | |
| $5_{0,5} \leftarrow 4_{0,4}$ | 28337.66 | −0.01 | −1.53 | |
| $5_{1,5} \leftarrow 4_{1,4}$ | 27536.70 | −0.05 | −0.97 | |
| $5_{2,4} \leftarrow 4_{2,3}$ | 28850.78 | 0.10 | −0.91 | |
| $5_{3,2} \leftarrow 4_{3,1}$ | 29037.33 | −0.14 | 0.25 | −0.01 |
| $6_{1,5} \leftarrow 5_{1,4}$ | 35932.73 | −0.07 | −4.16 | |
| $6_{2,4} \leftarrow 5_{2,3}$ | 35526.34 | −0.03 | −3.51 | |
| $6_{3,4} \leftarrow 5_{3,3}$ | 34839.93 | −0.12 | −0.85 | −0.01 |
| $6_{4,3} \leftarrow 5_{4,2}$ | 34808.60 | 0.07 | 1.51 | −0.04 |
| $6_{5,2} \leftarrow 5_{5,1}$ | 34784.69 | 0.13 | 4.52 | −0.09 |
| *b*-type | | | | |
| $7_{3,5} \leftarrow 7_{2,6}$ | 32050.60 | 0.10 | 1.35 | 0.08 |
| $9_{3,7} \leftarrow 9_{2,8}$ | 33473.84 | −0.03 | 2.09 | 0.05 |
| $11_{1,10} \leftarrow 11_{0,11}$ | 30622.32 | 0.00 | −31.73 | |
| $12_{3,9} \leftarrow 12_{2,10}$ | 23829.76 | −0.03 | 19.20 | −0.01 |
| $15_{3,12} \leftarrow 15_{2,13}$ | 24902.54 | −0.16 | −15.87 | −0.03 |
| $16_{4,12} \leftarrow 16_{3,13}$ | 33427.63 | −0.02 | 77.91 | −0.01 |
| $20_{4,16} \leftarrow 23_{3,20}$ | 31666.46 | −0.09 | −7.75 | −0.14 |
| $23_{4,19} \leftarrow 23_{3,20}$ | 37605.37 | 0.11 | −237.79 | 0.20 |
| $6_{1,6} \leftarrow 5_{0,5}$ | 36249.81 | 0.03 | −0.27 | |
| $7_{0,7} \leftarrow 6_{1,6}$ | 36535.40 | −0.05 | −5.35 | |
| *c*-type | | | | |
| $5_{3,2} \leftarrow 5_{2,4}$ | 31382.77 | −0.05 | −1.04 | 0.10 |
| $9_{3,6} \leftarrow 9_{2,8}$ | 34473.68 | −0.02 | −1.84 | 0.05 |
| $13_{4,10} \leftarrow 13_{3,10}$ | 37377.67 | −0.02 | 56.60 | 0.21 |
| $17_{4,14} \leftarrow 17_{3,14}$ | 26779.67 | 0.05 | 156.73 | −0.13 |
| $22_{5,18} \leftarrow 22_{4,18}$ | 35009.25 | −0.06 | 389.44 | −0.61 |
| $24_{5,20} \leftarrow 24_{4,20}$ | 27300.14 | −0.10 | 502.21 | −1.26 |
| $30_{6,25} \leftarrow 30_{5,25}$ | 30509.11 | 0.02 | 1096.68 | −4.43 |
| $31_{6,26} \leftarrow 31_{5,26}$ | 26071.43 | 0.06 | 1154.71 | −5.14 |
| $36_{7,30} \leftarrow 36_{6,30}$ | 33447.67 | −0.09 | 2081.65 | −12.23 |
| $38_{7,32} \leftarrow 38_{6,32}$ | 23848.11 | −0.02 | 2145.60 | −14.51 |
| $42_{8,35} \leftarrow 42_{7,35}$ | 36315.09 | −0.05 | 3587.23 | −28.84 |
| $43_{8,36} \leftarrow 43_{7,36}$ | 30929.85 | 0.15 | 3633.15 | −30.99 |
| $50_{9,42} \leftarrow 50_{8,42}$ | 28081.64 | −0.04 | 5638.41 | −65.50 |

[a] ±0.10 MHz.

*Table 8.* Spectroscopic constants[a,b] for the hydrogen-bonded *Gauche II* conformer of $H_2NCH_2CH_2CH{=}CH_2$.

| Vib. state | Ground | First ex. C2−C3 tors. | First ex. C3−C4[e] tors.[e] |
|---|---|---|---|
| N.o.t.[c] | 82 | 39 | 11 |
| R.m.s.[d]/MHz | 0.072 | 0.090 | 0.062 |
| $A_v$/MHz | 9109.934(12) | 9176.790(39) | 9151.15(45) |
| $B_v$/MHz | 3143.8879(54) | 3138.2418(81) | 3132.9662(66) |
| $C_v$/MHz | 2640.0207(54) | 2635.2717(82) | 2632.9848(62) |
| $\Delta_J$/kHz | 4.346(81) | 4.29(13) | 4.346[f] |
| $\Delta_{JK}$/kHz | −28.547(58) | −26.25(20) | −28.547[f] |
| $\Delta_K$/kHz | 77.5(13) | 68.4(35) | 77.5[f] |
| $\delta_J$/kHz | 1.3730(11) | 1.2566(48) | 1.373[f] |
| $\delta_K$/kHz | 6.985(60) | 6.94(20) | 6.985[f] |
| $\Phi_{JK}$/Hz | −0.435(89) | —[g] | —[g] |
| $\Phi_{KJ}$/Hz | −9.9(54) | —[g] | —[g] |
| $\Phi_K^h$/Hz | 177.(61) | —[g] | —[g] |

[a,b,c,d,e]Comments as for Table 4. [f]Kept constant at the ground-state value shown in the second column of this table. [g]Kept constant at zero in the least-squares fit. [h]Further sextic centrifugal distortion constants kept at zero; see text.

*Vibrationally excited states.* Two vibrationally excited states were assigned for this conformer, as indicated in Table 8. The spectroscopic constants of the first excited state of the C2−C3 torsional vibration were determined from 39 low-$J$ $^aR$- and medium-$J$ $^bQ$-branch transitions; no $c$-type $Q$-branch lines were strong enough to be identified beyond doubt. The frequency of this vibration was determined to be 83(20) $cm^{-1}$ by relative intensity measurements,[12] which is close to the value found for *Gauche I* above, as expected.

Only $^aR$-branch lines were sufficiently strong to be identified with certainty for what is probably the first excited state of the C3−C4 torsional vibration, or the lowest bending vibration. 11 transitions were used to determine the spectroscopic constants displayed in Table 8. The vibrational frequency is 148(30) $cm^{-1}$ for this mode, as determined by relative intensity measurements.[12]

*Dipole moment.* The dipole moment determined in the ordinary manner[18] is shown in Table 9. The total dipole moment of *Gauche II* is $3.972(75) \times 10^{-30}$ C m (Table 9). This is close to $3.92(4) \times 10^{-30}$ C m found for *Gauche I* (Table 6), as expected. The principal axis dipole moment components listed in Table 9 are close to the values calculated by the bond-moment method[13] (Table 1). This is one reason why it is presumed that the spectrum of Table 7 is that of *Gauche II.*

*Assignment of* Extended I. The assignments reported above include all the strongest lines of the spectrum, as well as a majority of lines of intermediate intensities and many weak transitions too. However, a rich spectrum of comparatively weak lines remained. Many of these last-mentioned transitions are undoubtedly associated with vibrationally excited states of the two *gauche* conformers which we were not able to assign, although many attempts were made with this in mind. From our work on $HSCH_2CH_2CH{=}CH_2$[8] it was known that *extended* conformers (see Figs. 2 and 3) might exist in such high concentrations that they could be detectable provided the H bonds of the two *gauche* conformers assigned above were not too strong. The asymmetry parameter $\varkappa$ for the three highly prolate *extended* conformers is about −0.995 in all three cases. The spectra of such highly prolate molecules are relatively easy to assign, provided that they have a sizable dipole moment component along the $a$-axis. This will give rise to characteristic $^aR$-branch $K_{-1}$-pile-ups. Unfortunately, none of the three *extended* rotamers are predicted to possess a large $\mu_a$, as can be inferred from Table 1. A search for such pile-ups was futile, as expected.

It can be seen from Table 1 that $\mu_c$ of *Extended I* is predicted to be comparatively large. Attempts to find this rotamer were therefore made next. The strongest transitions predicted for this

*Table 9.* Stark coefficients[a] and dipole moment[a] of the *Gauche II* conformer of $H_2NCH_2CH_2CH{=}CH_2$.

| Transition | | $\Delta\nu\ E^{-2}/10^{-6}$ MHz $V^{-2}$ cm$^2$ | |
|---|---|---|---|
| | | Obs | Calc |
| $5_{1,5} \leftarrow 4_{1,4}$ | $\lvert M\rvert = 1$ | −0.820(10) | −0.821 |
| | $\lvert M\rvert = 2$ | −0.415(6) | −0.421 |
| | $\lvert M\rvert = 3$ | 0.247(3) | 0.248 |
| $6_{2,5} \leftarrow 5_{2,4}$ | $M = 0$ | 1.69(2) | 1.61 |
| | $\lvert M\rvert = 1$ | 2.27(2) | 2.30 |
| | $\lvert M\rvert = 2$ | 4.17(5) | 4.30 |
| | $\lvert M\rvert = 3$ | 8.00(10) | 7.66 |
| $5_{2,3} \leftarrow 4_{2,2}$ | $M = 0$ | −1.20(2) | −1.22 |
| Dipole moment/$10^{-30}$ C m | | | |
| $\mu_a = 3.199(50)$ | $\mu_b = 1.211(93)$ | $\mu_c = 2.019(45)$ | $\mu_{tot} = 3.972(75)$ |

[a]Comments as for Table 6.

conformer are the *c*-type *Q*-branch $K_{-1} = 2 \leftarrow 1$ series starting in the upper frequency end of the spectrum and extending towards lower frequencies as the *J* quantum number increases. The starting value for *J* was predicted to be about 40 at 38 GHz, the upper end of the investigated frequency range. Moreover, the quadrupole coupling constants of *Extended I* (Table 2) predicted these transitions to be split by 0.7–0.9 MHz in a typical 1:2 intensity pattern. With this in mind, a search for the said *Q*-branch series was carried out. A search among the remaining, so far unassigned medium-intensity transitions displaying apparent quadrupole splittings was soon successful. The observed transitions are to be found in Table 10. There is no doubt about the assignment of these transitions as a *c*-type $K_{-1} = 2 \leftarrow 1$ series. The predicted quadrupole coupling constants (Table 2) conclusively demonstrate that this series indeed belongs to *Extended I,* because the quadrupole coupling constants predicted for the other two *extended* forms (Table 2) yield fine-structures completely different from those in Table 10.

However, a problem associated with the assignment of the *J* quantum numbers remains. The fact that *Extended I* is almost an accidental symmetrical top makes it difficult to decide whether a correct assignment of *J* has been made in Table 10. Several values of *J* can be successfully assumed for each transition, as judged by the least-squares fit. In an attempt to confirm the *J* assignments, searches were made for low-*J* *c*-type *R*-branch transitions. Unfortunately, there are only a few such transitions in the spectrum. They are considerably weaker than the identified *Q*-branch series and they are predicted to be split by quadrupole interactions in most cases. Our searches for them were therefore in vain. Attempts to find $^bQ$-branch transitions which might confirm the *J* assignments were also made, in spite of the fact that $\mu_b$ is predicted to be very small (Table 1). Not surprisingly, such series were not found.

The reason for selecting the tentative *J* assignments shown in Table 10 is that these values give the most reasonable values for the quartic and sextic centrifugal distortion constants shown in Table 11. Other values for the *J*'s yield much less realistic values for the centrifugal distortion constants than those shown in Table 11. With only one *Q*-branch series assigned, only $A_0 - C_0$ and the asymmetry parameter $\kappa$[16] can be determined (see Table 11). Only one quartic and one sextic centrifugal distortion constant were needed in order to obtain a root-mean-square deviation of the fit comparable to the experimental uncertainty. The "corrected" frequencies estimated using Rudolph's formula[20] were used in fitting these transitions to Watson's *A*-reduction *I*$^r$-representation Hamiltonian.[17] No problems were encountered with this Hamiltonian, even with such a prolate asymmetric rotor as this one.

No accurate values of both $\chi_{aa}$ and $\chi_{bb}$ can be

*Table 10.* Microwave spectrum[a] of the ground vibrational state of the *Extended I* conformer of $H_2NCH_2CH_2CH{=}CH_2$.

| Transition | $F' \leftarrow F''$ | Observed frequency[b]/MHz | "Corrected" frequency/MHz | Obs[c]–Calc frequency/MHz | Centrifugal distortion | |
|---|---|---|---|---|---|---|
| | | | | | Total/MHz | Sextic/MHz |
| $38_{2,37} \leftarrow 38_{1,37}$ | 39 ← 39 | 37898.68 | 37898.94 | −0.07 | −185.35 | 1.38 |
| | 37 ← 37 | | | | | |
| | 38 ← 38 | 37899.76 | | | | |
| $39_{2,38} \leftarrow 39_{1,38}$ | 40 ← 40 | 37244.58 | 37244.83 | 0.03 | −203.76 | 1.53 |
| | 38 ← 38 | | | | | |
| | 39 ← 39 | 37245.48 | | | | |
| $40_{2,39} \leftarrow 40_{1,39}$ | 41 ← 41 | 36577.98 | 36578.25 | 0.08 | −223.31 | 1.68 |
| | 39 ← 39 | | | | | |
| $42_{2,41} \leftarrow 42_{1,41}$ | 43 ← 43 | 35209.47 | 35209.70 | 0.02 | −265.90 | 2.03 |
| | 41 ← 41 | | | | | |
| | 42 ← 42 | 35210.44 | | | | |
| $43_{2,42} \leftarrow 43_{1,42}$ | 44 ← 44 | 34508.67 | 34508.90 | −0.01 | −288.92 | 2.22 |
| | 42 ← 42 | | | | | |
| | 43 ← 43 | 34509.62 | | | | |
| $44_{2,43} \leftarrow 44_{1,43}$ | 45 ← 45 | 33797.66 | 33797.89 | −0.04 | −313.08 | 2.42 |
| | 43 ← 43 | | | | | |
| | 44 ← 44 | 33798.59 | | | | |
| $45_{2,44} \leftarrow 45_{1,44}$ | 46 ← 46 | 33077.18 | 33077.40 | 0.03 | −338.37 | 2.64 |
| | 44 ← 44 | | | | | |
| | 45 ← 45 | 33078.05 | | | | |
| $46_{2,45} \leftarrow 46_{1,45}$ | 47 ← 47 | 32347.58 | 32347.81 | −0.10 | −364.76 | 2.87 |
| | 45 ← 45 | | | | | |
| | 46 ← 46 | 32348.52 | | | | |
| $48_{2,47} \leftarrow 48_{1,47}$ | 49 ← 49 | 30865.01 | 30865.25 | 0.10 | −420.64 | 3.36 |
| | 47 ← 47 | | | | | |
| | 48 ← 48 | 30865.88 | | | | |
| $49_{2,48} \leftarrow 49_{1,48}$ | 50 ← 50 | 30113.10 | 30113.34 | −0.05 | −450.04 | 3.63 |
| | 48 ← 48 | | | | | |
| | 49 ← 49 | 30113.92 | | | | |
| $50_{2,49} \leftarrow 50_{1,49}$ | 51 ← 51 | 29355.58 | 29355.78 | −0.02 | −480.33 | 3.91 |
| | 49 ← 49 | | | | | |
| | 50 ← 50 | 29356.37 | | | | |
| $51_{1,50} \leftarrow 51_{2,50}$ | 52 ← 52 | 28593.02 | 28593.22 | 0.00 | −511.31 | 4.20 |
| | 50 ← 50 | | | | | |
| $52_{2,51} \leftarrow 52_{1,51}$ | 53 ← 53 | 27826.34 | 27826.65 | −0.01 | −543.22 | 4.51 |
| | 51 ← 51 | | | | | |
| | 52 ← 52 | 27827.18 | | | | |

contd

*Table 10.* contd

| Transition | $F' \leftarrow F''$ | Observed frequency[b]/MHz | "Corrected" frequency/MHz | Obs[c]–Calc frequency/MHz | Centrifugal distortion | |
|---|---|---|---|---|---|---|
| | | | | | Total/MHz | Sextic/MHz |
| $53_{2,52} \leftarrow 53_{1,52}$ | $54 \leftarrow 54$<br>$52 \leftarrow 52$ | 27056.73 | 27056.85 | 0.11 | −576.63 | 4.83 |
| | $53 \leftarrow 53$ | 27057.31 | | | | |
| $54_{2,55} \leftarrow 54_{1,53}$ | $55 \leftarrow 55$<br>$53 \leftarrow 53$ | 26284.39 | 26284.65 | −0.07 | −608.54 | 5.16 |
| | $54 \leftarrow 54$ | 26285.31 | | | | |
| $59_{2,58} \leftarrow 59_{1,58}$ | $60 \leftarrow 60$<br>$58 \leftarrow 58$ | 22426.59 | 22426.77 | 0.00 | −775.96 | 6.97 |

[a]An ambiguity exists with regard to the quantum numbers involved in these transitions; see text. [b]±0.10 MHz. [c]"Corrected" frequency shown in preceding column used for least-squares fitting.

derived from the quadrupole splittings shown in Table 10 because the members of this $Q$-branch series have almost the same splittings for all transitions. There is thus not enough independent information to allow a determination of both $\chi_{aa}$ and $\chi_{bb}$. However, the quadrupole coupling constants shown in Table 2 predict splittings and intensity patterns very close to the observed ones.

*Assignment of* Extended II. It is seen from Table 1 that $\mu_b$ is predicted to be the largest principal axes dipole moment component for this conformer. This should result in a comparatively strong $b$-type $Q$-branch $K_{-1} = 1 \leftarrow 0$ series spreading out towards higher frequencies as $J$ increases. $J$ was predicted to be approximately 30 at 22 GHz and increasing with increasing frequency. The quadrupole coupling constants shown in Table 2 predicted unresolvable quadrupole splittings for this series provided it belonged to *Extended II*, whereas comparatively large splittings were predicted if it belonged to *Extended I*, and somewhat smaller splittings were predicted for this series in case it belonged to *Extended III*. The transitions displayed in Table 12 are undoubtedly a $b$-type $K_{-1} = 1 \leftarrow 0$ series, but because no further $Q$-branch series or $R$-branch lines were identified, the same ambiguity with respect to the $J$ quantum number exists for this conformation as in the case of *Extended I*, as reported above. The transitions of Table 12 were scrutinized for quadrupole splittings, but no such splittings were noted. This is one reason why the spectrum of this table is assigned to *Extended II*.

*Table 11.* Spectroscopic constants[a,b,c] of the ground vibrational state of the *Extended I* conformer of $H_2NCH_2CH_2CH=CH_2$.

| | |
|---|---|
| N.o.t. | 16 |
| R.m.s. dev./MHz | 0.067 |
| $(A_0-C_0)$/MHz | 16992.95(41) |
| $\varkappa$ | −0.995737 |
| $\delta_J$/kHz | −0.0943(11) |
| $\Phi_{JK}$/Hz | 0.21(20) |

[a]*A*-reduction I[r]-representation. [b]Using the quantum numbers shown in Table 10; see text. [c]Further centrifugal distortion constants preset at zero.

The derived spectroscopic constants are listed in Table 13. The tentative $J$ quantum numbers selected for the assignments shown in Table 12 were those that gave the most reasonable values for the centrifugal distortion constants, exactly as described above for *Extended I*. No determination of the dipole moment could be made for any of the two *extended* conformers assigned in this work due to the low intensity of the spectral lines as well as to the high-$J$ transitions assigned for both of them.

*Internal energy differences.* The internal energy differences were determined by comparison of spectral intensities. The principal axes dipole mo-

*Table 12.* Microwave spectrum[a] of the ground vibrational state of the *Extended II* conformer of $H_2NCH_2CH_2CH{=}CH_2$.

| Transition | Observed frequency[b]/MHz | Obs−calc frequency/MHz | Centrifugal distortion | |
|---|---|---|---|---|
| | | | Total/MHz | Sextic/MHz |
| $30_{1,29} \leftarrow 30_{0,30}$ | 22166.11 | 0.04 | 112.46 | −13.85 |
| $31_{1,30} \leftarrow 31_{0,31}$ | 22581.62 | 0.00 | 129.63 | −15.69 |
| $32_{1,31} \leftarrow 32_{0,32}$ | 23016.42 | −0.06 | 148.84 | −17.69 |
| $33_{1,32} \leftarrow 33_{0,33}$ | 23471.24 | 0.04 | 170.26 | −19.87 |
| $34_{1,33} \leftarrow 34_{0,34}$ | 23946.24 | −0.05 | 194.08 | −22.23 |
| $35_{1,34} \leftarrow 35_{0,35}$ | 24442.35 | 0.04 | 220.51 | −24.77 |
| $36_{1,35} \leftarrow 36_{0,36}$ | 24959.73 | −0.07 | 249.73 | −27.49 |
| $37_{1,36} \leftarrow 37_{0,37}$ | 25499.33 | 0.03 | 281.97 | −30.42 |
| $39_{1,38} \leftarrow 39_{0,39}$ | 26646.44 | −0.03 | 356.40 | −36.86 |
| $40_{1,39} \leftarrow 40_{0,40}$ | 27255.26 | 0.04 | 399.05 | −40.39 |
| $41_{1,40} \leftarrow 41_{0,41}$ | 27888.15 | 0.05 | 445.64 | −44.12 |
| $42_{1,41} \leftarrow 42_{0,42}$ | 28545.61 | −0.01 | 496.42 | −48.07 |
| $43_{1,42} \leftarrow 43_{0,43}$ | 29228.27 | 0.00 | 551.63 | −52.23 |
| $44_{1,43} \leftarrow 44_{0,44}$ | 29936.57 | 0.04 | 611.54 | −56.59 |
| $45_{1,44} \leftarrow 45_{0,45}$ | 30670.85 | 0.02 | 676.37 | −61.18 |
| $47_{1,46} \leftarrow 47_{0,47}$ | 33219.37 | 0.04 | 821.86 | −70.99 |
| $48_{1,47} \leftarrow 48_{0,48}$ | 33034.22 | −0.05 | 902.99 | −76.23 |
| $49_{1,48} \leftarrow 49_{0,49}$ | 33876.67 | −0.13 | 990.03 | −81.69 |
| $50_{1,49} \leftarrow 50_{0,50}$ | 34747.22 | 0.02 | 1083.20 | −87.38 |
| $51_{1,50} \leftarrow 51_{0,51}$ | 35645.74 | −0.01 | 1182.71 | −93.31 |
| $52_{1,51} \leftarrow 52_{0,52}$ | 36572.71 | 0.06 | 1288.76 | −99.48 |

[a,b]Comments as for Table 10.

ment components are crucial for the spectral intensities, and hence for the determination of internal energy differences between the conformers. Unfortunately, the dipole moment is not known for *Extended I* and *Extended II*. For these two rotamers, the predicted dipole moments shown in Table 1 were employed. It is also important to know the $J$ quantum numbers involved. As described above, an ambiguity exists for both the two *extended* forms with regard to this quantum number. The statistical weight was assumed to be 2 for all four conformers.

*Table 13.* Spectroscopic constants[a,b,c] of the ground vibrational state of the *Extended II* conformer of $H_2NCH_2CH_2CH{=}CH_2$.

| | |
|---|---|
| N.o.t. | 17 |
| R.m.s. dev./MHz | 0.061 |
| $(A_0-C_0)$/MHz | 16629.34(72) |
| $\kappa$ | −0.997462 |
| $\delta_J$/kHz | −0.12008(29) |
| $\Phi_{JK}$/Hz | −16.5(14) |

[a,c]Comments as for Table 11. [b]Using the quantum numbers shown in Table 12; see text.

The intensities of many transitions were compared in the limit of no power saturation.[21] *Gauche I* was found to be the most stable of them all. *Gauche I* is 0.8 kJ mol$^{-1}$ more stable than *Gauche II*. One standard deviation is liberally estimated to be ±0.3 kJ mol$^{-1}$. *Gauche I* is 1.9 kJ mol$^{-1}$ more stable than *Extended I*. One standard deviation is in this case liberally estimated to be ±0.5 kJ mol$^{-1}$. The uncertainties resulting from the unknown $\mu_c$-dipole moment component of *Extended I* as well as from the tentative $J$ quantum number assignment are taken into account. In an identical manner, *Gauche I* is found to be 2.1(5) kJ mol$^{-1}$ more stable than *Extended II*. These results are summarized in Table 17 and discussed below.

In addition to 1-amino-3-butene, the energy difference between the H-bonded *gauche* conformers and non-H-bonded conformers has been determined in one other case for the

$H_2NCH_2CH_2X$-type molecules in the free state, viz. for ethylenediamine,[22] where an energy difference of 1.9(5) kJ $mol^{-1}$ was determined using electron diffraction. However, this result is difficult to interpret because it represents some *mean* over two H-bonded *gauche* and several *anti* conformers.

*Searches for further conformers.* After these assignments had been made, there were only a few unassigned medium intensity transitions left in the spectrum. There is no reason to believe that *Extended III* has a much higher energy than the two other *extended* forms which were assigned. However, searches for this fifth rotamer were futile. One reason for this failure may perhaps be that none of its principal axes dipole moment components are as large as $\mu_c$ for *Extended I,* or $\mu_b$ for *Extended II* (see Table 1).

A search was also made for the hypothetical *Gauche III,* which has no H bond. A large $\mu_a$ is predicted for this conformation, as inferred from Table 1. However, no assignments could be made for this rotamer. This is not surprising, because *Gauche III* has no stabilizing H bond. In addition, the lone electron pair of the nitrogen nu-

*Table 14.* Plausible molecular structure[a] [bond lengths (pm), angles (°)] of $H_2NCH_2CH_2CH=CH_2$.

| | | | |
|---|---|---|---|
| Structural parameters kept fixed | | | |
| N–C4 | 147.5 | ∠C3–C4–N | 110.0[b] of 115.0[c] |
| C1–C2 | 133.1 | ∠C2–C3–C4 | 111.6 |
| C2–C3 | 149.6 | ∠C1–C2–C3 | 127.8 |
| C3–C4 | 152.8 | ∠C4–N–H | 107.0 |
| C1–H | 109.0 | ∠C3–C4–H | 109.47 |
| C2–H | 109.0 | ∠C4–C3–H | 109.47 |
| C3–H | 109.3 | ∠C2–C1–H | 121.5 |
| C4–H | 109.3 | ∠C1–C2–H | 121.5 |
| N–H | 101.7 | α(∠C1=C2–C3–C4) | 60.0 for *Extended* conformers[d] |
| | | β(∠C2–C3–C4–N) | 0.0 for *Extended* conformers[d] |
| Fitted[e] | | | |
| α(∠C1=C2–C3–C4) | | 66(3) for both *Gauche I* and *Gauche II* | |
| β(∠C2–C3–C4–N) | | 116(3) [64(3) from *syn*] for both *Gauche I* and *Gauche II* | |
| Hydrogen bond parameters | | | |
| Conformer: | | *Gauche I* | *Gauche II* |
| H[f]···C2 | | 257 | 270 |
| H[f]···C1 | | 297 | 313 |
| N···C2 | | 297 | 306 |
| N···C1 | | 357 | 369 |
| ∠N–H[f]···C2 | | 103 | 101 |
| ∠N–H[f]···C1 | | 118 | 116 |
| ∠N–H[f],C1=C2[g] | | 51 | 51 |
| Sum of van der Waals radii[h] | | | |
| H···C[i] | | 290 | |
| N···C[i] | | 320 | |

[a]See text. [b]Kept at this value for *Gauche I, Gauche II, Extended I,* and *Extended III.* [c]Kept at this value for *Gauche II* and *Extended II.* [d]This dihedral angle was not fitted for *Extended I* and *Extended II*; see text. [e]These two dihedral angles were fitted only for *Gauche I* and *Gauche II.* [f]Amino group hydrogen atom involved in intramolecular hydrogen bonding. [g]Angle between N–H bond involved in hydrogen bonding and C1=C2 bond. [h]Taken from Ref. 24. [i]Radius of aromatic carbon atom assumed to be 170 pm according to Ref. 24.

cleus of this conformation is oriented so that it is probably repelled by the π electrons of the double bond. *Gauche III* may thus perhaps represent a local maximum in the potential surface of 1-amino-3-butene. If this is the case, then there is no such thing as a stable *Gauche III* conformer.

Conformations other than the three *gauche* and three *extended* forms drawn in Figs. 2 and 3 are of course possible. *Syn* conformations (not shown in Figs. 2 and 3) which have a planar heavy-atom skeleton with $\alpha = 0°$, $\beta = 180°$, and $\gamma = 0°$ or $\gamma = 120°$ (see Fig. 1) were looked for, because it is known that a similar conformation occurs in large abundance in 1-butene.[19] These hypothetical *syn* conformations are predicted[13] to possess sizeable principal axes dipole moment components, and to be very crowded. However, no identification of them was made among the remaining unassigned, mostly rather weak transitions. It is impossible that large fractions of *syn* forms coexist with the two *gauche* and two *extended* conformers identified above for 1-amino-3-butene. It is concluded that the conformational make-up of 1-amino-3-butene primarily consists of two *gauche* conformers which are about 2 kJ $mol^{-1}$ more stable than the three *extended* rotamers.

*Structure.* As only one isotopic species has been investigated, insufficient data exist to perform a complete structure determination. Assumptions have to be made in order to derive important structural parameters. The C1C2C3C4 dihedral angle (α of Fig. 1) and the C2C3C4N dihedral angle (β of Fig. 1) were fitted for *Gauche I* and *Gauche II* in steps of 1°. These two parameters were fitted because they are chemically interesting and the rotational constants are sensitive to their variation. All the other structural parameters were kept constant in the fitting procedure at the values shown in Table 14. These parameters were selected from recent accurate studies of closely related compounds. It is noted that the C3C4N angle is assumed to be 110.0° when the dihedral angle γ of Fig. 1 is 0° or 240°, and 115.0° when γ is 120.0°. This relaxation of the CCN angle is discussed in Ref. 3.

The rotational constants are closely reproduced when the C1C2C3C4 dihedral angle (α) is 66° and the C2C3C4N dihedral angle (β) is 116° from *anti* (64° from *syn*) for both *Gauche I* and *Gauche II*, as shown in Table 15. The uncertainty limit corresponding approximately to three standard deviations is ±3° for both these dihedral angles. Note that β is practically identical to the corresponding values found for

*Table 15.* Observed and calculated rotational constants[a] of the *Gauche I* and *Gauche II* conformers of $H_2NCH_2CH_2CH{=}CH_2$.

| | *Gauche I* | | | *Gauche II* | | |
|---|---|---|---|---|---|---|
| | Obs | Calc[b] | Diff./% | Obs | Calc[b] | Diff./% |
| $A_0$/MHz | 9223.86 | 9244.87 | 0.22 | 9109.93 | 9154.41 | 0.49 |
| $B_0$/MHz | 3199.34 | 3210.38 | 0.34 | 3143.89 | 3151.29 | 0.23 |
| $C_0$/MHz | 2668.29 | 2671.06 | 0.10 | 2640.02 | 2648.84 | 0.33 |

[a]See text. [b]Structural parameters used in the calculations are found in Table 14.

*Table 16.* Observed and calculated spectroscopic constants[a] of the *Extended I* and *Extended II* conformers of $H_2NCH_2CH_2CH{=}CH_2$.

| | *Extended I* | | *Extended II* | |
|---|---|---|---|---|
| | Obs | Calc | Obs | Calc |
| $(A_0-C_0)$/MHz | 16992.95 | 17126.29 | 16629.34 | 17189.01 |
| κ | −0.99574 | −0.995117 | −0.99746 | −0.99689 |

[a,b]Comments as for Table 15.

*Table 17.* Selected results for three $XCH_2CH_2CH=CH_2$-type molecules.

| Molecule | $\alpha$[a]/degrees | $(\Delta E_0^\circ = E^\circ_{Extended} - E^\circ_{Gauche})$/kJ mol$^{-1}$ |
|---|---|---|
| $HOCH_2CH_2CH=CH_2$[b,c] | 75(3) | >3 |
| $H_2NCH_2CH_2CH=CH_2$[d] | 66(3)[e,f] | 1.9(5)[h] |
| | 66(3)[f,g] | 2.1(5)[i] |
| $HSCH_2CH_2CH=CH_2$[j] | 57(3) | 2.9(5)[k] |
| | | 3.6(6)[l] |

[a]Dihedral angle as defined in Fig. 1. [b]Ref. 7. [c]Ref. 23. [d]This work. [e]*Gauche I.* [f]Energy difference between *Gauche II* and *Gauche I* is 0.8(3) kJ mol$^{-1}$; see text. [g]*Gauche II.* [h]$E^\circ_{Extended\ I} - E^\circ_{Gauche\ I}$. [i]$E^\circ_{Extended\ II} - E^\circ_{Gauche\ I}$. [j]Ref. 8. [k]$E^\circ_{Extended\ I} - E^\circ_{Gauche}$. [l]$E^\circ_{Extended\ II} - E^\circ_{Gauche}$.

$HOCH_2CH_2CH=CH_2$[7,23] [116(3)°] and $HSCH_2CH_2CH=CH_2$[8] [115(3)°], while $\alpha$ is very different in the three cases, being 75(3)° in $HOCH_2CH_2CH=CH_2$[7], and 57(3)° in $HSCH_2CH_2CH=CH_2$,[8] in contrast to the value of 66(3)° found for both *Gauche I* and *Gauche II* (Table 14).

Due to the fact that the *J* quantum numbers are only tentative for *Extended I* and *Extended II* (see above), the spectroscopic constants also become uncertain. A fit of the dihedral angles $\alpha$, $\beta$ and $\gamma$ was therefore not considered to be worthwhile. However, only small adjustments of the said dihedral angles would reproduce $A_0 - C_0$ and $\varkappa$ rather well. The spectroscopic constants computed using the structural parameters of Table 14 assuming completely staggered atomic arrangements are listed in Table 16.

## Discussion

It was expected at the beginning of this work that the two H-bonded conformers *Gauche I* and *Gauche II* would be the most stable forms of 1-amino-3-butene, with *Gauche I* as the slightly more stable in accord with the findings made for the other $H_2NCH_2CH_2X$-type molecules.[1-6] This was indeed found, as demonstrated above. It is suggested that intramolecular H-bonding is the major cause of these conformational preferences. The H-bonds in *Gauche I* and *Gauche II* are rather weak, however, as can be inferred from the structural parameters and sums of the van der Waals radii[24] given in Table 14. It can also be seen from this table that the geometry of the H bond in *Gauche I* is only marginally different from that in *Gauche II*. The energy difference is, as expected, very small, being only 0.8(3) kJ mol$^{-1}$ in favour of *Gauche I*.

In order to compare the H-bond strengths in 3-butenes, selected data for the alcohol,[7,23] the thiol,[8] as well as for 1-amino-3-butene are collected in Table 17. The strength of the H bond is expected to manifest itself in at least two important parameters, viz. the C1C2C3C4 ($\alpha$) dihedral angle (see Fig. 1), and the energy difference between *extended* and *gauche* conformers. The H bond in the three compounds of Table 17 is undoubtedly strongest in $HOCH_2CH_2CH=CH_2$. This shows up in a large $\alpha$-angle of 75(3)° which brings the hydroxyl hydrogen atom and the $\pi$ electrons into close proximity, enhancing the hydrogen-bond interaction, as well in the fact that the energy difference between the H-bonded *gauche* conformer and any *extended* form is so large (over 3 kJ mol$^{-1}$) that the latter escaped being detected by electron diffraction[23] and MW spectroscopy.[7]

The strength of the H bond in *Gauche* $HSCH_2CH_2CH=CH_2$ as compared to the H bonds in *Gauche I* and in *Gauche II* of the title compound is more difficult to decide. The $\alpha$-angles are both about 9° larger in the two *gauche* rotamers of 1-amino-3-butene than in the H-bonded conformer of $HSCH_2CH_2CH=CH_2$[8] (Table 17). By this criterion, one would expect the H bond to be slightly stronger in both the *gauche* forms of $H_2NCH_2CH_2CH=CH_2$ than in *Gauche* $HSCH_2CH_2CH=CH_2$. However, the energy differences between the two *extended* forms and *gauche* conformer are both slightly larger in $HSCH_2CH_2CH=CH_2$ than in the corresponding three cases of $H_2NCH_2CH_2CH=CH_2$, as shown in Table 17. This fact should indicate the opposite

of what is found from the α dihedral angle, namely that the internal H bond is somewhat stronger in *Gauche* $HSCH_2CH_2CH=CH_2$ than in both *Gauche I* and *Gauche II* of 3-amino-1-butene. These findings make it impossible to say definitely whether the hydrogen bonds in the two *gauche* forms of the amine are stronger than in the thiol. It is then concluded that the H-bond strengths in *Gauche I* and in *Gauche II* are each nearly the same as in the H-bonded *Gauche* conformer of $HSCH_2CH_2CH=CH_2$.[8]

*Acknowledgments.* We are most grateful to Professor G. Courtois, *Laboratoire de Synthese Organique,* University of Poitiers, France, for the donation of the sample used in this work.

We would like to thank Otto for his interest in, and encouragement and support of MW spectroscopy over many years. Without his support there would hardly have been any MW spectroscopy in Norway.

## References

1. Marstokk, K.-M. and Møllendal, H. *Acta Chem. Scand., Ser. A 34* (1980) 15.
2. Braathen, O.-A., Marstokk, K.-M. and Møllendal, H. *Acta Chem. Scand., Ser. A 37* (1983) 493.
3. Braathen, O.-A., Marstokk, K.-M. and Møllendal, H. *Acta Chem. Scand., Ser. A 39* (1985) 209.
4. Marstokk, K.-M. and Møllendal, H. *J. Mol. Struct. 49* (1978) 221.
5. Caminati, W. and Wilson, E. B. *J. Mol. Spectrosc. 81* (1980) 356.
6. Caminati, W. *J. Mol. Spectrosc. 121* (1987) 61.
7. Marstokk, K.-M. and Møllendal, H. *Acta Chem. Scand., Ser. A 35* (1981) 395.
8. Marstokk, K.-M. and Møllendal, H. *Acta Chem. Scand., Ser. A 40* (1986) 615.
9. Courtois, G., Mesnard, D., Dugue, B. and Miginiac, L. *Bull. Soc. Chim. Fr.* (1987) 93.
10. Marstokk, K.-M. and Møllendal, H. *J. Mol. Struct. 5* (1970) 205.
11. Wodarczyk, F. J. and Wilson, E. B. *J. Mol. Spectrosc. 37* (1971) 445.
12. Esbitt, A. S. and Wilson, E. B. *Rev. Sci. Instrum. 34* (1963) 901.
13. Smyth, C. P. *Dielectric Behavior and Structure,* McGraw-Hill, New York 1955, p. 244.
14. Gordy, W. and Cook, R. L. *Microwave Molecular Spectra,* Wiley, New York 1984, p. 419.
15. Gordy, W. and Cook, R. L. *Microwave Molecular Spectra,* Wiley, New York 1984, p. 415.
16. Gordy, W. and Cook, R. L. *Microwave Molecular Spectra,* Wiley, New York 1984, p. 229.
17. Gordy, W. and Cook, R. L. *Microwave Molecular Spectra,* Wiley, New York 1984, p. 329.
18. Marstokk, K.-M. and Møllendal, H. *Acta Chem. Scand., Ser. A 36* (1982) 517.
19. Kondo, S., Hirota, E. and Morino, Y. *J. Mol. Spectrosc. 28* (1968) 471.
20. Rudolph, H. D. *Z. Naturforsch., A 23* (1968) 540.
21. Townes, C. H. and Schawlow, A. L. *Microwave Spectroscopy,* McGraw-Hill, New York 1955, p. 372.
22. Kazerouni, M. R., Barkowski, S. L., Hedberg, L. and Hedberg, K. *Proceedings of the Eleventh Austin Symposium on Molecular Structure,* Austin, Texas 1986, p. 33.
23. Trætteberg, M. and Østensen, H. *Acta Chem. Scand., Ser. A 33* (1979) 491.
24. Pauling, L. *The Nature of the Chemical Bond,* 3rd ed., Cornell University Press, New York 1960, p. 260.

Received October 25, 1987.